Chapter 6

Characterization of the *jamb* and *jamc* mutant phenotypes

Summary

In this chapter I describe the phenotype of mutant embryos homozygous for the *jamb*^{HU3319} nonsense allele or the *jamc*^{sa0037} missense allele. Disruption of either gene results in a complete lack of myoblast fusion, characterized by mononuclear fast-twitch muscle fibres with a striking regimented arrangement of centrally-positioned nuclei with respect to myotome boundaries. Mutant mononuclear fibres differentiate fully, as determined by expression of fast muscle myosin heavy chain, but appear to be delayed; the elongation of each fibre and concomitant arrangement of nuclei is not evident until approximately 32 h. p. f. There is a 1.8-fold and 1.6-fold increase in the number of fast muscle fibres in *jamb* and *jamc* mutant embryos, respectively. These phenotypic characteristics are inconsistent with the *Drosophila* founder cell paradigm of myoblast fusion, suggesting a different vertebrate-specific regulatory mechanism is used for this process.

6.1 Introduction

Loss-of-function experiments are crucial to the study of any biological system. The functions of JAM-B and JAM-C in mouse have been well-characterised using targeted knockout mutants generated through homologous recombination (see Chapter 1). Unfortunately, this technique is not yet available for the study of gene function in zebrafish.

Forward genetics screens were of key importance to the identification of critical genes involved in the early development of zebrafish (Driever *et al*, 1996). Briefly, chemical mutagenesis generated many mutant lines identified from assaying phenotypic defects in a biology of interest, for example, muscle motility (Granato *et al*, 1996). The causative allele of a given mutant is then later identified by positional cloning. This process is lengthy and resource intensive, but yields important long-term tools and relevant functional information. For example, the *candyfloss* mutant identified from a screen of muscle motility mutants (Granato *et al*, 1996) has been used to better understand the pathology of a major subgroup of congenital muscular dystrophies (CMD), the *laminin α2*-deficient CMD (MDC1A; Hall *et al*, 2007). Forward genetics screens are primarily limited by the difficulty of screening large numbers of embryos with ever more complicated phenotypic assays to identify rare phenotypes or mutations. With increasingly cheaper sequencing and the availability of complete genome sequences, more targeted reverse genetics methods for generating non-functional alleles are now widely used. Targeting Induced Local Lesions IN Genomes (TILLING) is an established method in zebrafish, first designed for use in studying *Aradopsis thaliana* (McCallum *et al*, 2000) and subsequently adapted for other organisms. Briefly, male zebrafish are chemically mutagenised and then mated to wild-type females to yield a library of F1 progeny. Genomic DNA is taken from F1 fish and analysed for mutations within a gene of interest by PCR and sequencing. Identified heterozygous carrier F1 fish are then outcrossed as many times as may be required to isolate the mutation of interest from other 'background' mutations, which may be closely linked. The random mutagenesis of an individual genome can result in an allelic series for a given gene from a single screen. However, disruption of haploinsufficient genes and mutations that result in a dominant lethal phenotype cannot be isolated by TILLING. Other reverse genetic methods which use different means of random mutagenesis have been developed, for example, retroviral insertions (Wang *et al*, 2007) or transposon-mediated gene trapping (Kawakami *et al*, 2004). These techniques require maintenance of large libraries of fish and are also resource intensive, making them less suitable for small scale laboratories.

A more recently developed genetic method for targeted loss-of-function in zebrafish makes use of customised zinc finger nucleases (ZFN; reviewed in Urnov *et al*, 2010), originally applied to *Drosophila melanogaster* (Bibikova *et al*, 2002). Briefly, customised proteins, containing three zinc finger domains and the catalytic domain of FokI nuclease, are designed to bind specific inverted 9 base pair DNA sequences flanking a site of interest, separated by 4-6 base pairs. FokI nuclease is only active upon dimerisation. Once bound to both sites within the genomic DNA, in the correct orientation, the FokI domains can dimerise and induce a double-strand break. Repair of this lesion by non-homologous end joining can result in a small insertion or deletion that disrupts the targeted gene. This is an exciting technology, with a potential for gene modification or addition through homology-directed repair. The main drawback, however, is the lengthy and complicated process to produce specific nucleases that are active *in vivo* and have the desired effect of yielding a targeted mutant line.

In the absence of rapid genetic methods for gene disruption in zebrafish, morpholinos have been widely used in functional studies (reviewed in Bill *et al*, 2009). Morpholinos are antisense oligonucleotides in which the phosphoribose backbone has been replaced with a phosphorodiamidate backbone. This modification yields higher affinity binding to RNA and prevents enzymatic degradation of the oligomer *in vivo*. Morpholinos are injected into zebrafish embryos to block the translation or splicing of a specific target mRNA. The oligomer binds to the translation start site or a splice donor site, inhibiting translation or splicing by steric hindrance. While morpholinos have proved to be useful reagents, there has been considerable difficulty in controlling toxicity and off-target binding effects (reviewed in Eisen and Smith, 2008). Previously, a morpholino targeting *jamc*[1] was included in a functional screen of cell surface and secreted proteins in zebrafish (Pickart *et al*, 2006). The morpholino-injected embryos displayed a marked defect in pigmentation. At 24 h. p. f., morpholino-injected embryos lacked differentiated melanophores until approximately 48 h. p. f. No other phenotype was described for this morpholino. It is important to note, however, that only 15 of the 25 nucleotides of the sequence are found to match the very 5′ end of the annotated *jamc* 5′ UTR. No full-length matches were identified through BLAST searches of the entire nucleotide collection at the NCBI. Given these difficulties, it is highly unlikely that this phenotype is a result of the

[1] This morpholino was incorrectly annotated as targeting *jam2* (referred to here as *jamb*). A BLAST search of the morpholino sequence against the zebrafish genome reveals its target as *jamc*. It is not similar to any other zebrafish *jam* family members.

loss-of-function of *jamc*.

To get the best and most unequivocal results of loss-of-function studies of *jamb* and *jamc*, I sought out TILLING mutants from two different resources available to other zebrafish researchers: the Hubrecht Laboratory and the Wellcome Trust Sanger Institute Zebrafish Mutation Resource. Very shortly after obtaining these mutants, it became obvious that loss-of-function of both genes results in a near-complete loss of myoblast fusion. To highlight the phenotypic consequences of disruption of myoblast fusion genes in different model organisms, I will briefly describe results from functional studies of the guanine exchange factor *myoblast city* (*mbc*) in *Drosophila* and its orthologues *Dock1* and *Dock5* in zebrafish and mouse.

Loss-of-function of *mbc* in *Drosophila* results in a complete block of myoblast fusion (Rushton *et al*, 1995). All null alleles of *mbc* are recessive and embryonic lethal, as the mutant larvae are unable to hatch from the vitelline membrane. Within the hemisegment of a *mbc* mutant larvae, there are two phenotypically different populations of unfused myoblasts. One is a large population of rounded, myosin-expressing myoblasts that are phagocytosed by macrophages, decreasing in number from around 13 hours after egg laying (AEL). The other is a small population of myoblasts that also express myosin, but persist until 17 hours AEL, migrate to positions of body wall muscles and elongate and attach to the epidermis. These sub-populations are referred to as fusion-competent myoblasts (FCMs) and founder cells, respectively (see Chapter 1).

In contrast, morpholino knockdown of zebrafish homologues *dock1* or *dock5* results in a significant increase in mononucleate fibres at 26 – 28 h. p. f., but the majority of myocytes elongate to span each somite (Moore *et al*, 2007). Simultaneous knockdown of *dock1* and *dock5* does not result in any significant enhancement of the phenotype of either morpholino used individually. This suggests that disruption of both genes only partially suppresses myoblast fusion.

Investigation of *Dock1* null embryos in mouse reveals a similar phenotype. At embryonic day 13.5 – 14.5 the majority of myosin heavy chain-expressing fibres are elongated and mononuclear throughout the embryo (Laurin *et al*, 2008). Primary myoblasts isolated from embryonic day 18.5 *Dock1* null mice reveal a significant defect in myoblast fusion in culture; 80% of desmin-expressing *Dock1* null myoblasts remain mononucleate, in contrast to 20% of wild-type myoblasts. It is important to note, however, that the isolated null primary myoblasts remained rounded in cell culture, but elongate and align to form muscle bundles in the embryo. The *Dock1* null allele is lethal, likely because newborn pups fail to breathe. In contrast, a *Dock5* null

allele is viable and seems morphologically normal. However, an incompletely penetrant muscle phenotype was observed in *Dock1*$^{+/-}$, *Dock5*$^{-/-}$ embryos, suggesting some functional redundancy between the orthologues.

Clearly, *myoblast city* activity in myogenesis is conserved between invertebrates and vertebrates, and is critical for myoblast fusion. However, the phenotypic consequences of loss-of-function are different in the different models. Upon blocking myoblast fusion in the vertebrate models, the majority of myocytes elongate and form mononucleate fibres, but only a rare sub-population do so in fruitflies. This suggests a different, vertebrate-specific process for fusion. The gross phenotypic consequences of disrupting myoblast fusion between the vertebrate models highlights the relative merits and drawbacks of studying muscle development in zebrafish. Importantly, the accessibility and translucence of zebrafish embryos makes it easy to detect and quantify myoblast fusion defects in the embryo *in situ*. In mice, studies of myoblast fusion have largely been limited to extraction of primary myoblasts or immortalised myoblast cell lines which might not behave the same in culture (Cornelison, 2008). Interestingly, very few studies of genes reported as playing a role in myoblast fusion in cell culture have demonstrated any effect of gene disruption in the embryo. For example, M-cadherin has been implicated in myoblast fusion in cell culture (Charrasse *et al*, 2007), but no similar phenotype has been described in M-cadherin null embryos (Hollnagel *et al*, 2002). It is worth noting, however, that simultaneous knockdown of *dock1* and *dock5* in zebrafish didn't completely disrupt myoblast fusion, unlike the *Dock1*$^{-/-}$ or *Dock1*$^{+/-}$, *Dock5*$^{-/-}$ embryos, suggesting the genes involved and their relative roles in this process may be different between vertebrate models.

To understand the function of *jamb* and *jamc* during muscle development, I characterised the development of the axial musculature in wild-type, *jamb*^{HU3319} and *jamc*^{sa0037} zebrafish embryos. Myoblast fusion was completely blocked in both mutants, resulting in an overabundance of fast muscle fibres. These results suggest that Jamb and Jamc act as a receptor:ligand pair, and that the majority of myoblasts are able to form muscle fibres. This observation is inconsistent with the founder cell paradigm for myoblast fusion, suggesting a different vertebrate-specific mechanism.

6.2 General characteristics of the *jamb*^{HU3319} and *jamc*^{sa0037} alleles and mutants

Mutant alleles of *jamb* and *jamc* were isolated from two separate TILLING screens. The *jamb*^{HU3319} allele, identified and supplied by the Hubrecht Institute

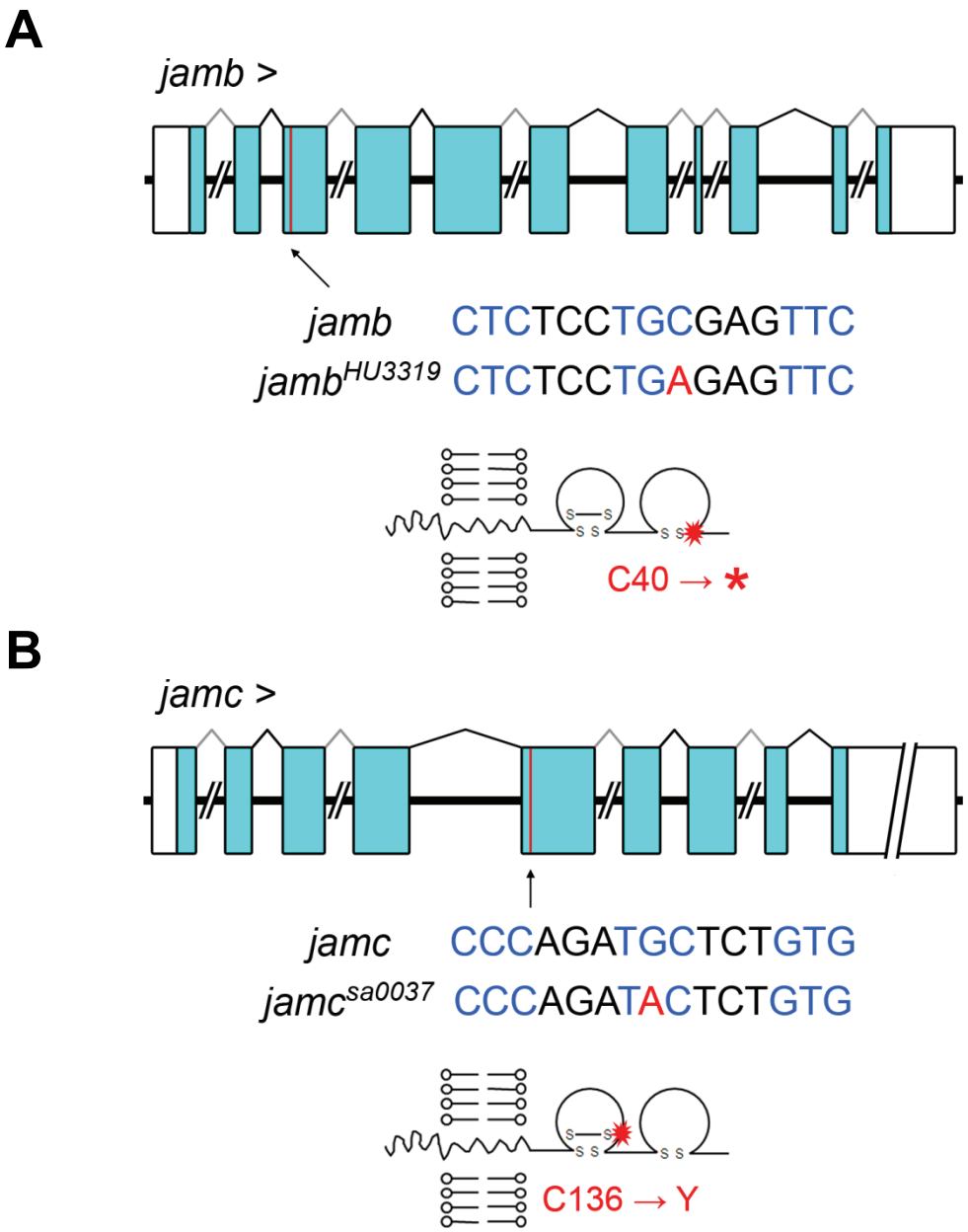

Figure 6.1 The molecular nature of *jamb*^{HU3319} and *jamc*^{sa0037} alleles.

A. Diagram illustrating the structure of the *jamb* loci. The *jamb*^{HU3319} allele contains a nonsense mutation in exon 3 (red line), introducing a stop codon (shown below the diagram) and truncating the protein (schematic below sequence) in the membrane-distal immunoglobulin-like domain (red star). **B.** Diagram illustrating the structure of the *jamc* loci. The *jamc*^{sa0037} allele contains a missense mutation in exon 5, changing a codon encoding cysteine to a codon encoding tyrosine (shown below the diagram) and disrupting a conserved disulphide bond in the membrane-proximal immunoglobulin-like domain (red star, schematic below sequence). Diagrams are drawn to scale; introns or untranslated regions larger than 400 bp were truncated for clarity, as indicated.

(Utrecht, Netherlands), contains a nonsense mutation in exon 3 of *jamb* (figure 6.1). The premature stop codon truncates the Jamb protein in the B β-strand of the N-terminal immunoglobulin-like domain (figure 6.1). This mutation results in a complete lack of Jamb expression, as determined by immunohistochemistry (figure 6.2) using a polyclonal antibody raised against the extracellular domain of Jamb. The *jamc*^{sa0037} allele, isolated from a library raised at the Wellcome Trust Sanger Institute Zebrafish Mutation Resource (Hinxton, U. K.), contains a missense mutation in exon 5. This alters the codon for cysteine-136 to tyrosine (figure 6.1). The mutation disrupts the non-canonical, but conserved, disulphide bridge between Cys-136 and Cys-222 on the A and G β-strands of the membrane-proximal immunoglobulin-like domain. It is reasonable to assume that this disruption would seriously affect the folding and function of Jamc and the allele was subsequently shown to be a strong hypomorph.

Mutant embryos homozygous for either allele are viable and fertile in our aquarium, but do not thrive. There is significant transmission bias of either allele, likely because of poor survival of homozygote embryos, although the gross morphology of 5 day larvae before transfer to the aquarium is normal. Current generations of *jamc*^{sa0037} adult fish grow slowly and present a wide range of morphological defects, unlike *jamc*^{sa0037}/+ siblings, suggesting the existence of other recessive background mutations. Female *jamc*^{sa0037} adults become egg-bound quickly without regular spawning and male *jamc*^{sa0037} adults seem reluctant or unsuccessful mates; spawning events are often spread over a long time period from initial light stimulus. Size and fertilization rates of clutches do not appear different between mutant and wild-type fish. Adult *jamb*^{HU3319} fish appear normal in gross morphology and behaviour. Initial breeding of *jamb*^{HU3319}/+ fish identified a recessive pigment defect, but this was not linked to *jamb* genotype (figure 6.3 and table 6.1).

6.3 *jamb*^{HU3319} and *jamc*^{sa0037} mutants display a complete block in myoblast fusion

Both *jam* mutant embryos show a near complete lack of myoblast fusion in the fast muscle myotomes along the trunk and tail, as highlighted by labelling of all cell membranes by transient expression of membrane-targeted red fluorescent protein (mRFP; figure 6.4). At 48 h. p. f. mutant fast muscle is composed of mononuclear fibres with a characteristic arrangement of nuclei equidistant from either myotome boundary, in stark contrast to the multinucleated wild-type myofibres. This phenotype is not evident in mutants until approximately 32 h. p. f. (figure 6.4) and persists until at least 5 days (figure 6.5). Embryos injected with morpholinos that prevent the

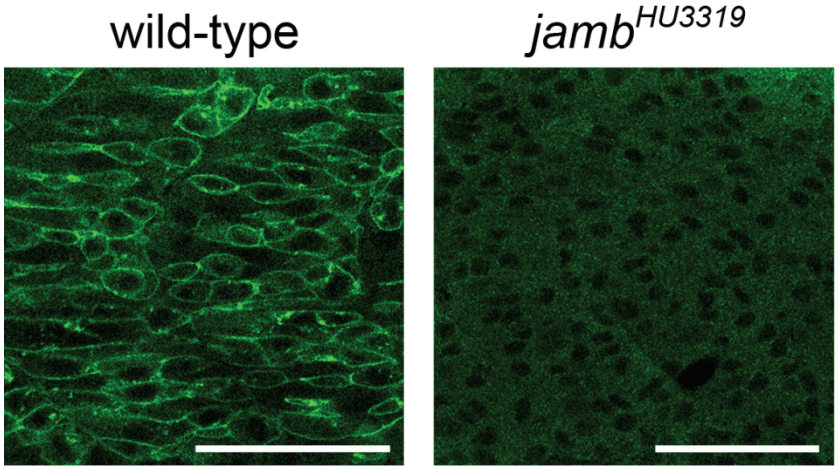

Figure 6.2 Jamb is not detected in *jamb*^{HU3319} mutant embryos.

Immunohistochemistry against Jamb (green) detects the protein on the cell surface of myoblasts and myotubes in wild-type, but not *jamb*^{HU3319} mutant, siblings. Confocal microscopy images of mid-trunk somites of 21 somites stage siblings from a *jamb*^{HU3319}/+ incross. Anterior left; scale bars represent 50 μm.

Figure 6.3 A pigment defect in *jamb*^{HU3319}/+ incross progeny is recessive.

Microscopy images of examples of *jamb*^{HU3319}/+ incross progeny at 48 h. p. f., showing normal pigmentation in 75% of embryos and an apparent lack of melanin pigmentation (*pig*) in the remaining 25%, suggesting a causative recessive mutation. This phenotype is not observed in all *jamb*^{HU3319}/+ incross clutches, suggesting it is not caused by the *jamb*^{HU3319} allele.

Table 6.1 Pigment defect is not linked to *jamb*^{HU3319} allele. Percent frequency of *jamb* genotype and pigment defect phenotype in embryos from a single *jamb*^{HU3319}/+ incross clutch.

Phenotype	Genotype			Total
	wild-type	*jamb*^{HU3319}/+	*jamb*^{HU3319}	
wild-type	17.3%	38.5%	19.2%	75%
unpigmented	3.8%	15.4%	5.8%	25%
Total	21.1%	53.9%	25%	100%

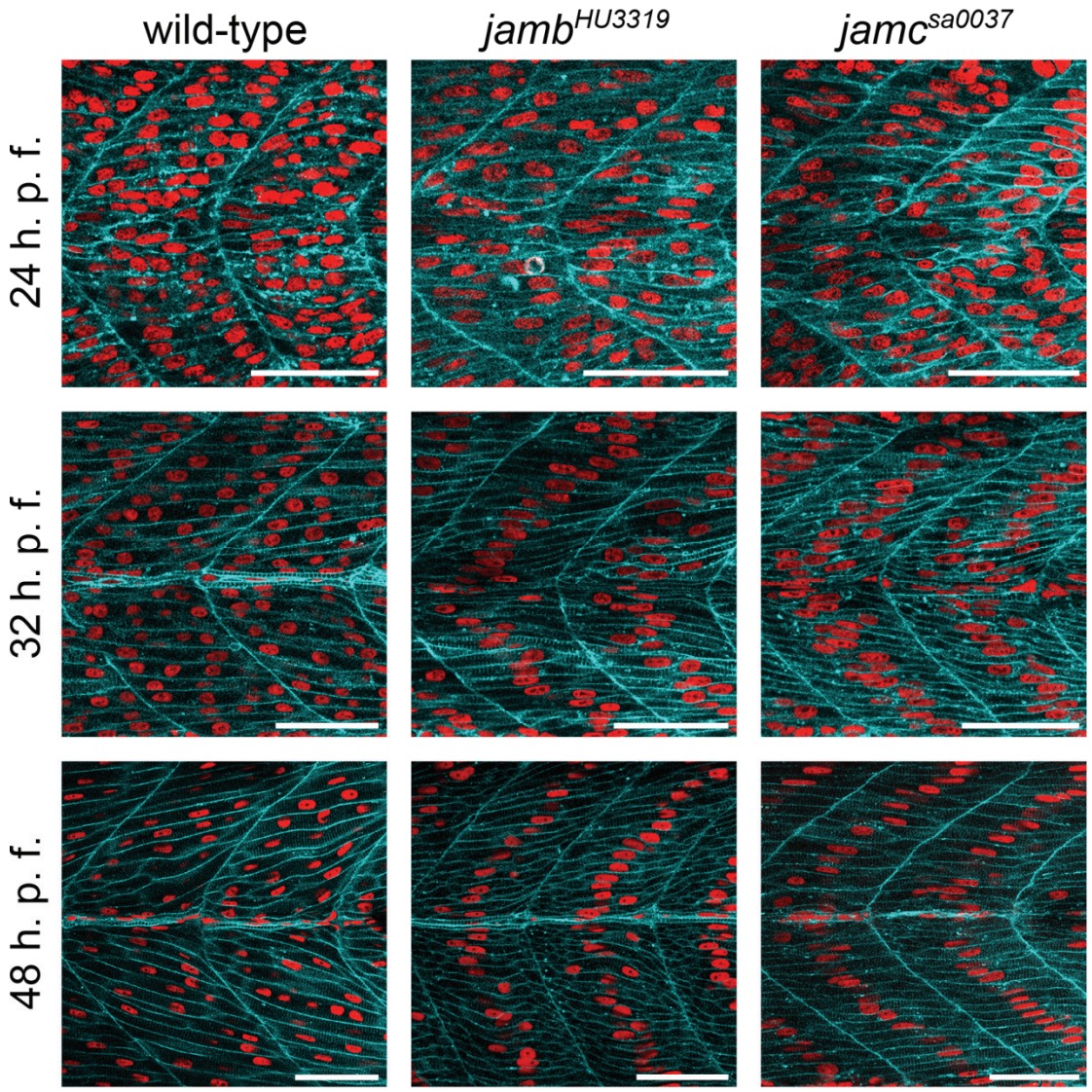

Figure 6.4 Fast muscle fibres are mononuclear in *jamb*^{HU3319} and *jamc*^{sa0037} mutants.

Confocal microscopy images of myotomes 12-13 in wild-type, *jamb*^{HU3319} and *jamc*^{sa0037} mutant embryos at 24 h. p. f. (top row), 32 h. p. f. (middle row) and 48 h. p. f. expressing membrane-targetted RFP (cyan) and counterstained with DAPI to highlight nuclei (red). In wild-type embryos, most myoblasts have fused to form multinucleated fast muscle fibres which thicken and express sarcomeric proteins. In both *jamb*^{HU3319} and *jamc*^{sa0037} mutants, most myoblasts have elongated by 24 h. p. f., but appear undifferentiated until approximately 32 h. p. f., at which time, fast muscle fibres thicken and a characteristic chevron arrangement of nuclei becomes evident. Anterior left; scale bars represent 50 μm.

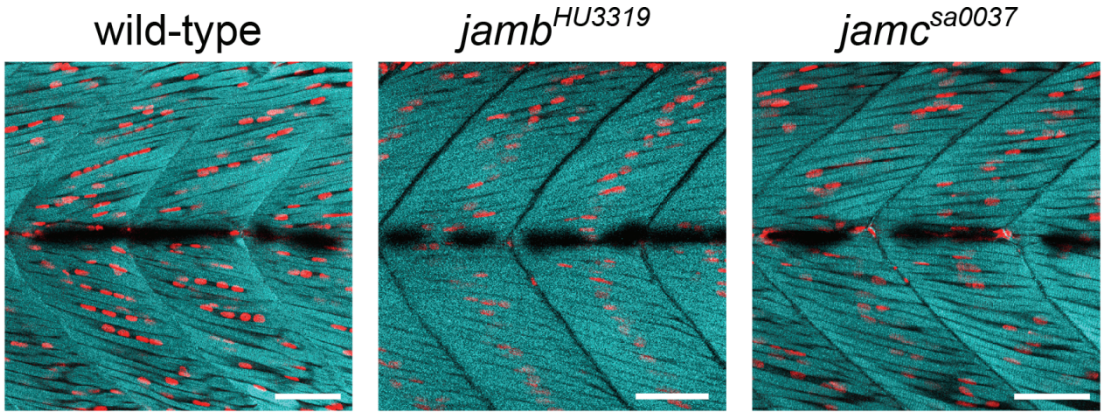

Figure 6.5 Fast muscle fibres are mononuclear in 5 day old *jamb*^{HU3319} and *jamc*^{sa0037} mutants

Mononuclear fast muscle fibres persist until at least 5 days of development. Confocal microscopy images of myotomes 12-13 in wild-type, *jamb*^{HU3319} and *jamc*^{sa0037} mutant embryos at 120 h. p. f., stained for F-actin (cyan) and nuclei (red) with phalloidin-Alexa 488 and DAPI, respectively. Anterior left; scale bars represent 50 µm.

translation of either gene, phenocopy the mutants (figure 6.6), demonstrating that the phenotype can be attributed to the *jamb*^{HU3319} and *jamc*^{sa0037} mutant alleles and not another mutation closely linked to either allele. The phenotype does not result from an overabundance of axial slow muscle, which is mononucleate in zebrafish (Roy *et al*, 2001), as the number and position of slow muscle fibres is the same as wild-type, as determined by immunohistochemistry against slow muscle myosin heavy chain (sMyHC; figure 6.7). As expected, mutant mononuclear fibres express fast muscle myosin heavy chain (fMyHC) and are supernumary compared to wild-type (figure 6.8). Muscle fibre differentiation is delayed in mutant embryos by several hours because elongated fibres are not evident until approximately 32 h. p. f., 6-8 hours after wild-type embryos (figure 6.4).

6.4 Fast muscle fibres are overabundant in *jamb*^{HU3319} and *jamc*^{sa0037} mutants

To quantify the overabundance of fast-twitch myofibres, I counted mRFP-labelled fast muscle fibres in optical cross-sections of wild-type and mutant embryos between 24-48 h. p. f (figure 6.9 and table 6.2; see Chapter 2). There is a statistically significant increase of myofibre number by approximately 1.8 and 1.6 -fold in *jamb*^{HU3319} and *jamc*^{sa0037} embryos, respectively, at 32 and 48 h. p. f., compared to wild-type (tables 6.2 and 6.3). The difference between the two mutants is likely because of the hypomorphic nature of the *jamc*^{sa0037} allele. Subsequent experiments demonstrate that approximately 5% and 15% of fibres are multinucleate in *jamb*^{HU3319} and *jamc*^{sa0037} embryos, respectively, compared to 97% in wild-type embryos (see Chapter 7, table 7.1: *jamb*^{HU3319} donor, *jamb*^{HU3319} host, *jamc*^{sa0037} donor, *jamc*^{sa0037} host and wild-type donor, wild-type host). These results show that in the absence of myoblast fusion, the majority of myoblasts are able to undergo differentiation to form functional muscle fibres.

6.5 Myoblast proliferation is repressed in *jamb*^{HU3319} and *jamc*^{sa0037} embryos

The average number of nuclei in each fibre at 48 h. p. f. in wild-type embryos is approximately 3 (Moore *et al*, 2007). In light of this result, one would expect a much higher number of mononucleate fibres in both mutants compared to wild-type. One possible explanation for the apparent lack of fast muscle fibres is apoptosis of unfused myoblasts in mutant embryos. To assess this, wild-type, *jamb*^{HU3319} and *jamc*^{sa0037} embryos were treated with acridine orange between 24 and 32 h. p. f.

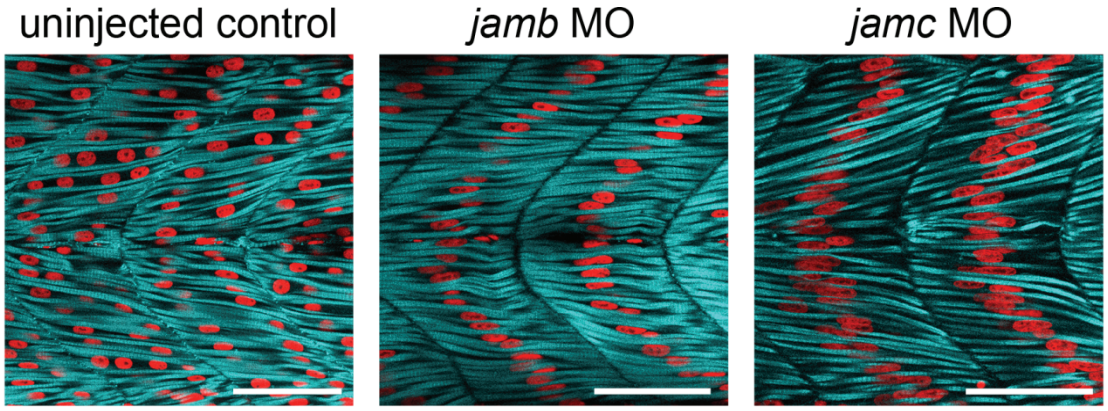

Figure 6.6 Morpholinos targeted to *jamb* and *jamc* phenocopy mutant alleles.

Confocal miscroscopy images of myotomes 12-13 in uninjected, *jamb* and *jamc* morpholino-injected wild-type embryos at 48 h. p. f., stained for F-actin (cyan) and nuclei (red) with phalloidin-Alexa 488 and DAPI, respectively. Anterior left; scale bars represent 50 µm.

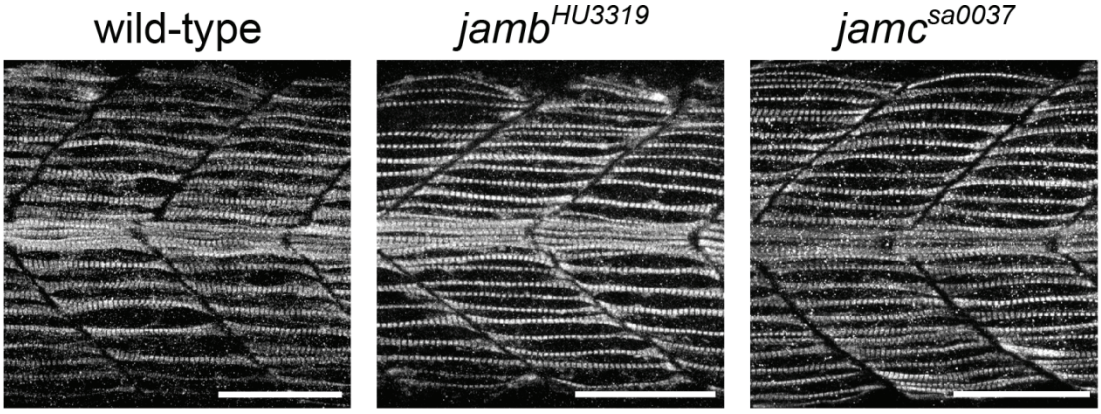

Figure 6.7 Slow muscle develops normally in *jamb*^{HU3319} and *jamc*^{sa0037} mutants.

Confocal microscopy images of myotomes 12-13 in wild-type, *jamb*^{HU3319} and *jamc*^{sa0037} 24 h. p. f. embryos, stained for slow muscle-specific myosin heavy chain (sMyHC). Slow muscle is superficial and develops normally in both mutants compared to wild-type. Anterior left; scale bars represent 50 μm.

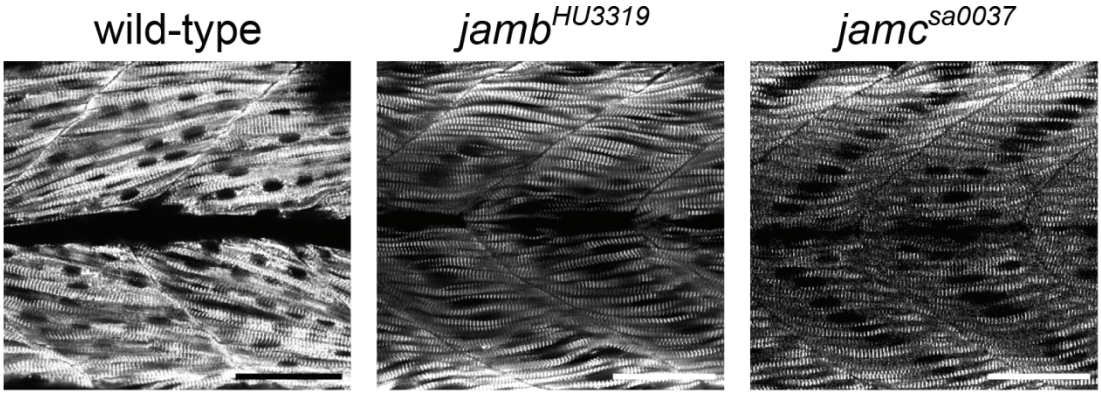

Figure 6.8 Fast muscle fibres are fully differentiated in *jamb*^{HU3319} and *jamc*^{sa0037} mutants.

Confocal microscopy images of myotomes 12-13 in wild-type, *jamb*^{HU3319} and *jamc*^{sa0037} 48 h. p. f. embryos, stained for fast muscle-specific myosin heavy chain (fMyHC). Mononucleate fast muscle fibres are differentiated and supernumary in both mutants compared to wild-type. Anterior left; scale bars represent 50 μm.

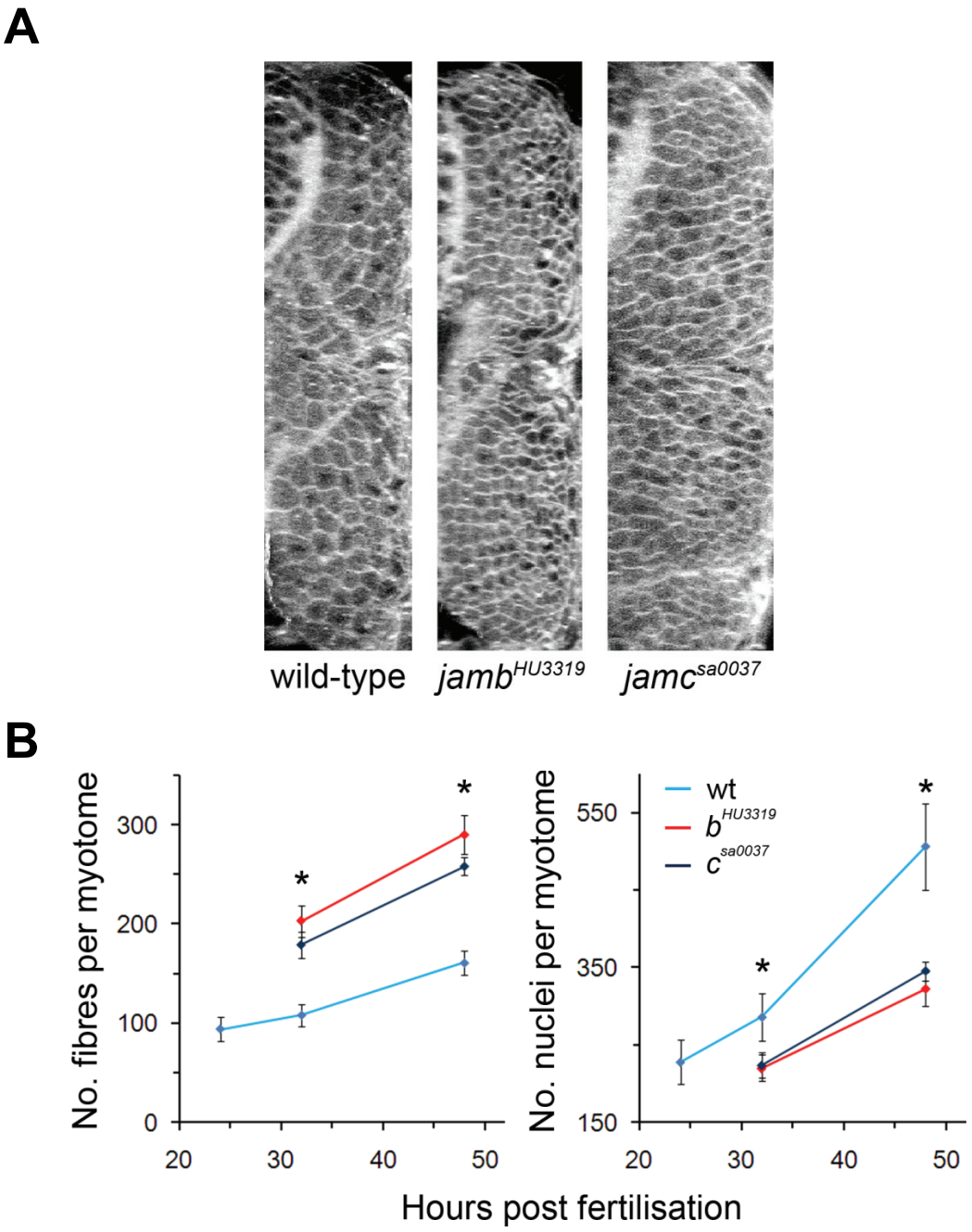

Figure 6.9 Quantification of supernumary fast muscle fibres in both *jamb*^{HU3319} and *jamc*^{sa0037} mutant embryos.

A. Cross-sections of myotomes from wild-type, *jamb*^{HU3319} and *jamc*^{sa0037} 48 h. p. f. embryos expressing membrane-targetted RFP (mRFP). Images were generated from confocal microscopy z-stack images. Dorsal, top. **B.** Graphs showing the average number of fast muscle fibres per myotome at different stages of development (left) and the estimated average number of nuclei per myotome at different stages of development (right) in wild-type, *jamb*^{HU3319} and *jamc*^{sa0037} embryos. Error bars represent standard deviation.

Table 6.2 Quantification of number of fast muscle fibres per myotome in wild-type, *jamb*^{HU3319} and *jamc*^{sa0037} embryos. Average number of fast muscle fibres per myotome in wild-type and mutant embryos at different developmental stages. Values presented as mean ± S. D., n = number of embryos tested.

Time (h. p. f.)	Genotype							
	wild-type		*jamb*^{HU3319}			*jamc*^{sa0037}		
	no. fibres	n	no. fibres	ratio to wt	n	no. fibres	ratio to wt	n
24	94 ± 12	12	-	-	-	-	-	-
32	108 ± 11	10	203 ± 16	1.9	6	179 ± 13	1.7	5
48	159 ± 17	8	290 ± 20	1.8	11	258 ± 9	1.6	6

Table 6.3 Statistical significance of comparisons between fast muscle fibre number in wild-type, *jamb*^{HU3319} and *jamc*^{sa0037} embryos. One-tailed probability values from t-tests adjusted to account for unequal variances and sample sizes.

Time (h. p. f.)	Comparison		
	wild-type – *jamb*^{HU3319}	wild-type – *jamc*^{sa0037}	*jamb*^{HU3319} – *jamc*^{sa0037}
32	2.0×10^{-6}	2.2×10^{-5}	0.01
48	3.7×10^{-12}	1.3×10^{-9}	2.4×10^{-4}

There was no qualitative increase in apoptosis observed in mutants compared to wild-type embryos (figure 6.10).

Another possible explanation is a reduction of myoblast proliferation in mutant embryos after the completion of primary myogenesis at 24 h. p. f. The rate of increase in fibre number is the same in mutant and wild-type embryos between 32 – 48 h. p. f. (figure 6.9), yet the number of fast muscle fibre nuclei must increase much more quickly in wild-type embryos than mutants, as each new muscle fibre requires many more myoblasts. To address this possibility I estimated the relative numbers of nuclei per myotome and developmental stage (figure 6.9, tables 6.4 and 6.5). The number of fast muscle fibres at each stage (f_h, where h represents developmental stage, h. p. f.) was multiplied by the average number of nuclei per fibre (n_h), reported in Moore *et al* (2007). This number was adjusted for the percentage of multinucleate fibres (m) observed in subsequent transplant experiments (wild-type - 97%, *jamb*^{HU3319} – 5%, *jamc*^{sa0037} – 15%; see Chapter 7) as follows:

$$\text{number of nuclei per myotome} = mf_h n_h + (1 - m)f_h$$

As expected, there is a statistically significant difference in the number of nuclei per myotome in wild-type embryos compared to both mutants, and this difference increases over time. These results suggest there is a decrease in myoblast proliferation in both *jamb*^{HU3319} and *jamc*^{sa0037} mutant embryos. Thus, while there is a clear overabundance of fast muscle fibres in both *jam* mutants, this increase is smaller than expected because of limited myoblast proliferation.

6.6 Discussion

Both *jamb*^{HU3319} and *jamc*^{sa0037} mutant embryos display the same phenotype: delayed, overabundant, mononucleate fast muscle fibres in the axial musculature. This phenotype is recapitulated in morpholino knockdown embryos, indicating it is specific to the loss-of-function of either gene. These results demonstrate that Jamb and Jamc are likely to be a vertebrate-specific receptor:ligand pair and are necessary for fusion between myoblasts during primary myogenesis in the zebrafish myotome. Further experiments performed to test this hypothesis are described in Chapter 7.

The differences in phenotype between myoblast fusion mutants in *Drosophila* and the *jam* mutants reveal interesting differences in the process of muscle development. In *Drosophila*, early specification of rare muscle founder cells determines the absolute number and nature of muscles formed in each hemisegment, irrespective of the occurrence of myoblast fusion (Ruiz-Gomez *et al*, 2000). In contrast, the absence of myoblast fusion in either *jam* mutant results in an

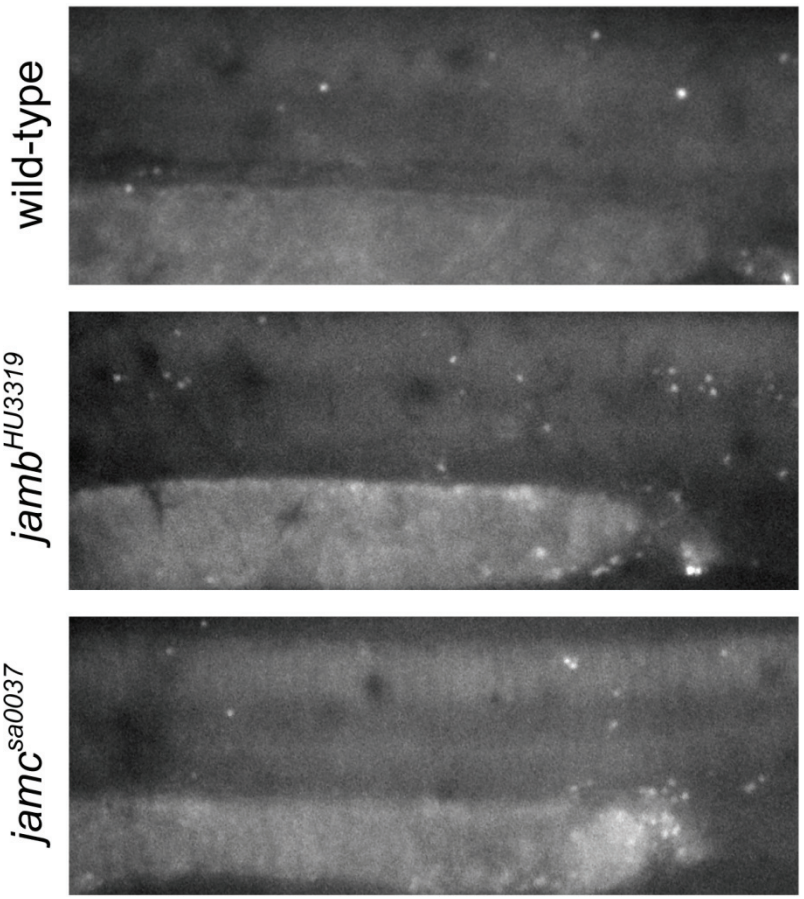

Figure 6.10 Apoptosis does not increase in the absence of myoblast fusion.

Example images of wild-type, *jamb*^{HU3319} and *jamc*^{sa0037} mutant embryos incubated in acridine orange at 32 h. p. f. showing no qualitative increase in mutant embryos relative to wild-type. Anterior left.

Table 6.4 Calculated number of nuclei per myotome in wild-type, *jamb*^{HU3319} and *jamc*^{sa0037} embryos. Average number of nuclei per myotome, calculated from number of fast muscle fibres per myotome in wild-type and mutant embryos at different developmental stages. Values presented as mean ± S. D., number of embryos tested as in table 6.2.

Time (*h*; h. p. f.)	Average no. nuclei per fibre (n_h)*	Genotype				
		wild-type	*jamb*^{HU3319}		*jamc*^{sa0037}	
		no. nuclei	no. nuclei	ratio to wt	no. nuclei	ratio to wt
24	2.48	228 ± 29	-	-	-	-
32	2.70	286 ± 30	220 ± 17	0.8	224 ± 16	0.8
48	3.23	506 ± 56	322 ± 22	0.6	345 ± 12	0.7

* Values from Moore *et al*, 2007

Table 6.5 Statistical significance of comparisons between number of nuclei per myotome in wild-type, *jamb*^{HU3319} and *jamc*^{sa0037} embryos. One-tailed probability values from t-tests adjusted to account for unequal variances and sample sizes.

Time (h. p. f.)	Comparison		
	wild-type – *jamb*^{HU3319}	wild-type – *jamc*^{sa0037}	*jamb*^{HU3319} – *jamc*^{sa0037}
32	4.2×10^{-5}	1.1×10^{-4}	0.35
48	1.1×10^{-5}	5.0×10^{-5}	7.2×10^{-3}

increase in the number of fast muscle fibres. This suggests that in zebrafish myogenesis, the majority, if not all, myoblasts are capable of forming a myofibre. While the overabundance of fast muscle fibres is clear, it is not as high as might be expected in light of the average number of nuclei in wild-type myotome. There is no obvious increase in apoptosis of myoblasts before differentiation, discounting this as a possible explanation. An analysis of muscle fibre growth suggests a reduction of myoblast proliferation in mutants compared to wild-type over time, which might explain the apparent lack of fibres. It is difficult to speculate on a link between proliferation of dermomyotome cells, which are likely to be the source of new myoblasts for myotome growth (Hammond *et al*, 2007), and myoblast fusion mediated by *jamb* and *jamc*. One possibility that remains to be assessed is whether proliferation of mutant myoblasts before differentiation results in an excess of fast muscle fibres. Differentiation of mutant myoblasts is delayed by approximately 6 – 8 hours compared to wild-type. Whether or not these cells are post-mitotic or proliferative during this delay is unknown.

Another important aspect of regulation in *Drosophila* is the more ubiquitous fusion competent myoblast population. They act as a substrate that fuses to muscle founders to increase the bulk of each fibre (Ruiz-Gomez *et al*, 2002). In the absence of fusion they persist as rounded cells, weakly express myosin heavy chain and eventually undergo apoptosis (Rushton *et al*, 1995). Similarly, in zebrafish *kirrel* morpholino-injected embryos, a large population of myoblasts fail to form fibres, remain rounded, express myosin heavy chain although how long these cells persist, or if they do form mononucleate fibres is uncertain (Srinivas *et al*, 2007). These cells are described as being lateral to slow muscle fibres, possibly impeding their migration from the midline to a lateral superficial position. However, no such phenotype was observed in either $jamb^{HU3319}$ or $jamc^{sa0037}$ mutants. It is difficult to rationalise the difference in phenotype between *kirrel* morpholino-injected embryos and both *jam* mutants. One possibility is that the *kirrel* morpholino directly affects the development of slow muscle, as noted by Srinivas *et al* (2007), and this in turn affects the development of fast muscle myoblasts (Henry and Amacher, 2004). Whilst appropriate controls were performed by the authors of the study of *kirrel*, the possibility of toxic side-effects of injected morpholinos remains to be fully explored in this context. It would be interesting to establish the veracity of the morpholino phenotype by using a loss-of-function allele, but none have been reported to date.

In summary, characterisation of mutant alleles of *jamb* or *jamc* show that a loss-of-function of either gene results in a complete block of myoblast fusion. As a

consequence, the majority of myoblasts within each somite form a mononucleate fibre, resulting in a significant overabundance of fast muscle. These results are not consistent with a founder cell model of myogenesis, in which the number of muscle fibres remains constant in the absence of fusion because each of them is predefined by a rare sub-population of 'founder' cells.